Journal of Molecular Modeling (2025) 31:299
https://doi.org/10.1007/s00894-025-06517-2

ORIGINAL PAPER

Antioxidant and chelating properties of phenolic compounds of agro-industrial waste of *Carapa guianensis*: theoretical insights for food and pharmaceutical applications

Neidy S.S. dos Santos[1] · Loubenky Surfin[1] · William Silva[1] · Antonio Rodrigues da Cunha[2] · Herbert Georg[3] · Kaline Coutinho[4] · Sylvio Canuto[4] · Rodrigo Gester[5]

Received: 21 April 2025 / Accepted: 15 September 2025 / Published online: 16 October 2025

Abstract

Context This study investigates the antioxidant behavior and chelating properties of thirteen phenolic compounds identified in *Carapa guianensis* agro-industrial waste. Using quantum mechanical methods, we analyzed the molecular structure and solvent effects, revealing potential applications in the food and pharmaceutical industries. Approximately 85% of these compounds demonstrated superior antioxidant performance compared to the phenol backbone, with three compounds rivaling quercetin and ascorbic acid in all tested environments. Solvent polarity significantly influenced the antioxidant mechanism: while hydrogen atom transfer (HAT) dominated in the gas phase, sequential proton loss electron transfer (SPLET) became prevalent in polar solvents. Hydrogen abstraction occurred primarily at the *meta* position, though polar solvents increased activity at the *para* site. These predictions are confirmed by simulating the chemical reactions between the aromatic compounds and free OH radicals. The analysis of the hydrogen abstraction reactions indicates that the inclusion of Hartree-Fock exchange-correlation and dispersion corrections is essential to describe hydrogen abstraction by explicitly free radicals. These findings not only underscore the commercial potential of *Carapa guianensis* waste but also provide a comprehensive understanding of its antioxidant mechanisms, contributing to the sustainable use of natural resources for health and environmental benefits.

Methods This is a two-step methodology. First, we select the best antioxidant molecules through thermochemical analysis. Then, we explore the hydrogen scavenging mechanism using transition state theory. All quantum mechanics and thermodynamic analyses were carried out within the framework of the density functional theory using the M06-2X, ωB97, ωB97XD, and CAM-B3LYP variants associated with the Pople's 6-311++G(d, p) basis set. The effects of the solvent are also systematically investigated by considering the Solvent Density Model for different polar and nonpolar environments. Naturally, the unrestricted wave-function formalism is accounted for once the thermodynamic description of the antioxidant mechanisms involves optimizing open-shell structures. Additionally, the chemical reaction of the hydrogen abstraction due to OH radicals is ensured by applying the Synchronous Transit-Guided Quasi-Newton Method, which allows us to estimate the transition state structures and the energy barrier of the reaction. At this stage, DFT methods like CAM-B3LYP and ωB97XD were applied in association with the 6-31+G(d). All calculations were carried out taking advantage of the Gaussian 16 program.

Keywords Antioxidants · Phenolic compounds · Reaction mechanisms · Polar solvents · Agro-industrial waste

Introduction

Free radicals are highly harmful compounds that cause premature aging and contribute to diseases such as arteriosclerosis, Alzheimer's, and Parkinson's [1, 2]. Antioxidants, which

✉ Neidy S.S. dos Santos
neidysamara@gmail.com

✉ Rodrigo Gester
gester@unifesspa.edu.br

[1] Programa de Pós-Graduação em Química, Universidade Federal do Sul e Sudeste do Pará, Marabá 68507-590, Brazil

[2] Universidade Federal do Maranhão, Balsas 65800-000, Brazil

[3] Instituto de Física, Goiânia 74690-900, Brazil

[4] Instituto de Física, Universidade de São Paulo, Rua do Matão 1371, São Paulo 05588-090, Brazil

[5] Faculdade de Física, Universidade Federal do Sul e Sudeste do Pará, Marabá 68507-590, Brazil

neutralize free radicals through hydrogen dissociation, are beneficial to living organisms and have become crucial for the cosmetic, pharmaceutical, and food industries [3]. As a result, finding new eco-friendly sources of antioxidants is essential. Agro-industrial wastes have emerged as an important alternative, offering a sustainable and low-cost solution [4–6]. These wastes are rich in bioactive compounds, with applications in the food industry, biogas, biofuel production, and as a potential source of antioxidants.

For agro-economy-based countries, exploring the financial potential of agro-wastes can provide significant advantages. In this context, species like *Carapa guianensis* emerge as promising candidates. This medicinal plant, abundant in the Amazon biome, exhibits remarkable versatility, being used as a larvicide, repellent, and therapeutic agent due to its anthelmintic properties [7–10]. Beyond its therapeutic applications, *Carapa guianensis* serves as a source of raw materials for biodiesel production and holds economic importance in South America, Asia, and Africa.

However, the potential of its agro-industrial wastes remains underexplored, with few initiatives such as that by Santos and co-workers [11], who were among the first to identify all phenolic constituents in this biomass using metabolomic techniques. Additionally, andiroba biomass has demonstrated significant antioxidant activity against DPPH and ABTS free radicals, with IC_{50} values of 16.42 μg/mL and 6.52 μg/mL, respectively [11].

In the search for new drug sources, molecular modeling and quantum chemical approximations have significantly contributed by predicting the antioxidative potential of chemophores and elucidating the mechanisms of these chemical reactions. Hydrogen abstraction can occur through three primary routes: hydrogen atom transfer (HAT), sequential proton loss electron transfer (SPLET), and sequential electron transfer-proton transfer (SET-PT) [12–14].

Thus, the goal is to use quantum mechanics and molecular modeling techniques to calculate formation enthalpies, characterize hydrogen abstraction, and determine the most favorable antioxidant mechanism. This methodology has been used as the first theoretical approach for quantifying antioxidant performances and determining the molecular site for hydrogen abstraction [15–17]. In the second stage, it is important to determine the activation energies for hydrogen scavenging, considering the explicit interaction between the reference molecule and free radicals like OH, OOH, and DDPH [18–23].

Given the context outlined above, we conducted a systematic quantum chemical and thermodynamic investigation of the antioxidant behavior of *Carapa guianensis* agro-industrial constituents. The results align with previous experimental data for some compounds found in andiroba waste, confirming the accuracy of our conclusions. Dissociation energies were compared with phenol and ascorbic acid, demonstrating that andiroba waste is a reliable and efficient source of antioxidants. Additionally, the solvent plays a crucial role, influencing the behavior of phenolic compounds and shifting the antioxidant mechanism with increasing polarity.

Methodology

Our main goal is to investigate the antioxidant behavior of the thirteen phenolic compounds previously identified in *Carapa guianensis* agro-industrial wastes and signalize possible applications (see Fig. 1). This analysis is entirely based on quantum mechanical and thermochemical parameters like enthalpy. The theory and procedure are better described in previous works [18, 24]. The proton (H^+), electron (e), and hydrogen ($H^\bullet$) enthalpies, we used the current values found in the literature [25, 26]

In addition, phenolic compounds retain the ability to chelate ions of transition metals, in accordance with the Transition Metal Chelation (TMC) mechanism [27, 28]. Once the chelation usually occurs through deprotonated hydroxyl groups in phenolic compounds, the capacity of one molecule to give away a proton is assumed as $ArOH \rightarrow ArO^- + H^+$. From the thermochemical point of view, the gas-phase acidity is computed as the difference between the enthalpies of the anion and its neutral species as [13]

$$\Delta H_{acidity} = H_{ArO^-} - H_{ArOH} \tag{1}$$

For the condensed phase, the acidities are obtained in terms of total free solvation energies like

$$\Delta G_{acidity} = G_{ArO^-} - G_{ArOH} \tag{2}$$

All molecular geometries were optimized using density functional theory (DFT) with the M06-2X/6-311++G(d, p) method. This functional was chosen based on the work by Souza and Peterson, which showed its superior correlation with accurate coupled-cluster models compared to other DFT methods [29]. The minimum-energy configurations were obtained by scanning the orientations of the hydrogen bonds formed by the hydroxyl groups (OH). This step is crucial because the hydrogen bond orientation can significantly affect molecular stability [8]. Similarly, we scanned the molecular potential energy surface to determine the optimal orientations of the carbon chains attached to the aromatic rings. All quantum mechanics calculations were performed on these minimized energy structures (Fig. 2).

The solvent effects of benzene ($\varepsilon = 2.3$) and water ($\varepsilon = 78.4$) were simulated using the solvent model density (SMD) [30]. In addition to the general advantages of continuum

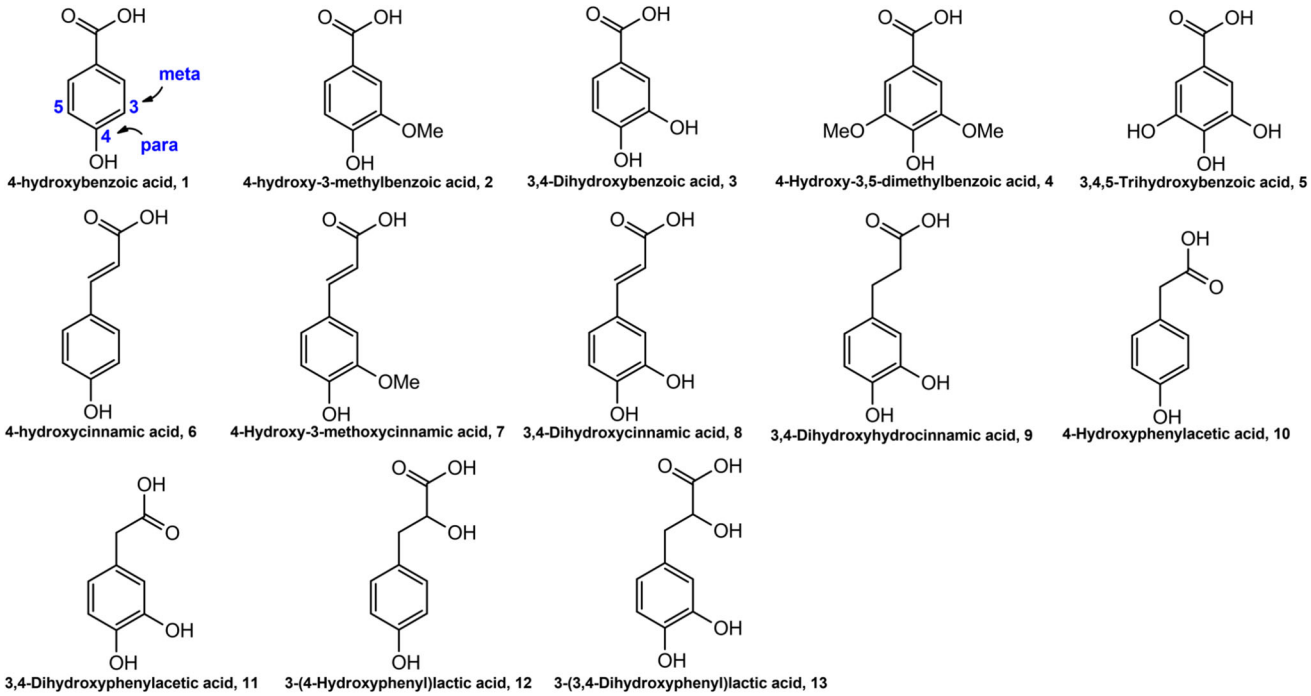

Fig. 1 Phenolic acids present in the agro-industrial wastes of andiroba oil

solvation models, SMD provides precomputed electron, proton, and hydrogen enthalpies for various wavefunction-based methods and DFT functionals, including the M06-2X Hamiltonian [26, 31, 32]. Hydrogen scavenging was analyzed using a quantum mechanics approach to chemical kinetics. Reagents and products were optimized using the unrestricted CAM-B3LYP and ωB97XD methods with the 6-31+G(*d*) basis set, widely used in reaction mechanism studies [21–23]. The transition states were located using the quasi-Newton method guided by synchronized transit [33]. For dispersion-corrected DFT methods, we employed Grimme's D3 correction with Becke-Johnson damping (GD3-BJ), which has been shown to provide reliable thermochemical properties [34]. In the absence of sufficient experimental data, we adopted the benchmark results of de Souza and Peterson, who demonstrated using high-level CCSD(T) calculations that the M06-2X functional offers optimal performance for polyphenolic systems [35]. While M06-2X proved accurate, its significant computational cost prompted us to additionally evaluate CAM-B3LYP. For our dispersion interaction analysis, we selected the ωB97 and ωB97XD functionals based on their established performance and computational efficiency, with ωB97XD being particularly recommended as a robust choice by Goerigk and Grimme [36]. The ωB97XD functional was also preferred due to its widespread implementation in major quantum chemistry packages such as Gaussian and Dalton. All quantum mechanics calculations were performed using Gaussian 16 software [37].

Results

HAT mechanism

From the electronic structure, it is possible to predict where the hydrogen atom will be extracted. By an analysis of the highest occupied and lowest unoccupied molecular orbitals (HOMO and LUMO), it is expected that the abstraction will occur at the hydroxyl group that is covered by the HOMO but is out of the LUMO. As an example, in Fig. 3, one expects that the hydrogen abstraction would happen at the *meta* position. However, no amount of energy is known about the amount of energy necessary to remove these atoms.

The hydrogen atom transfer (HAT) mechanism, governed by bond dissociation energies (BDEs), is the simplest hydrogen abstraction process. The BDEs are presented in Table 1. As shown in Fig. 1, some compounds (3, 5, 8, 9, and 11) feature multiple hydroxyl groups at *meta* (3-OH) and *para* (4-OH) positions. The results reveal a strong dependence on hydroxyl position, with a preference for hydrogen abstraction at the *meta* position. For instance, under gaseous conditions, compound 3 exhibits BDE values of 341.2 kJ/mol (3-OH) and 376.8 kJ/mol (4-OH), a difference of 35.6 kJ/mol. Lower BDE values indicate easier hydrogen extraction and higher antioxidant potential.

These findings align with the spin density analysis in Fig. 2a. Generally, a lower spin population on the O-atom correlates with lower BDEs and greater antioxidant power

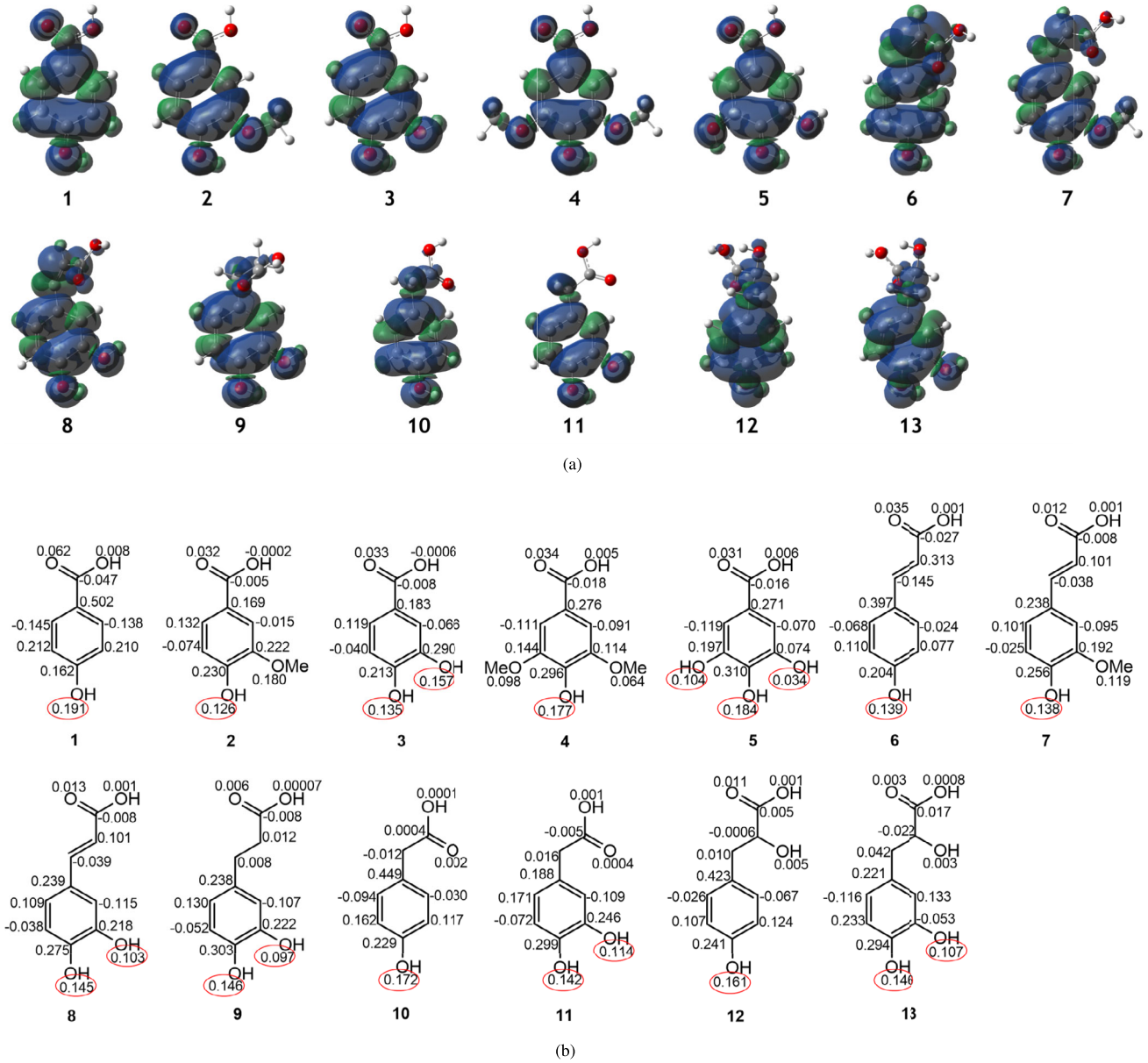

Fig. 2 Spin density isosurfaces (**a**) and its projections at each atomic site (**b**) calculated using the DFT/M06-2X/6-311++G(*d*, *p*) approcimation level in aqueous

[38, 39]. This trend holds for all phenolic derivatives with OH groups at *meta* and *para* positions (5, 8, 9, 11, and 13), except for compound 3. For example, Fig. 2b shows spin density values of 0.097 (*meta*) and 0.172 (*para*) for compound 9.

Although the energy difference is significant, the solvent reduces the barrier between these enthalpies. As shown in Table 1, the difference decreases from the gas phase to 29 kJ/mol (benzene) and 10.5 kJ/mol (water). This effect is more pronounced for compound 8, where the difference drops from 22.6 kJ/mol (gas phase) to 18.1 kJ/mol (benzene) and 2.3 kJ/mol (water). Increasing solvent polarity makes it difficult to determine whether hydrogen abstraction occurs at *meta* or *para* sites. Additionally, including explicit solvent molecules and specific interactions, such as solute-solvent hydrogen bonds, can further minimize this energy difference in water. For example, Guedes et al. studied the differential solvation of phenol and phenoxy radical [40, 41], finding that the solute-solvent interaction energies differ by less than 8 kJ/mol from benzene to acetonitrile [41].

To evaluate the antioxidant performance of phenolic derivatives, their behavior is compared to phenol, the foundational structure for these compounds [13, 42, 44]. Table 1 and Fig. 4 present these comparisons using $\Delta BDE =$

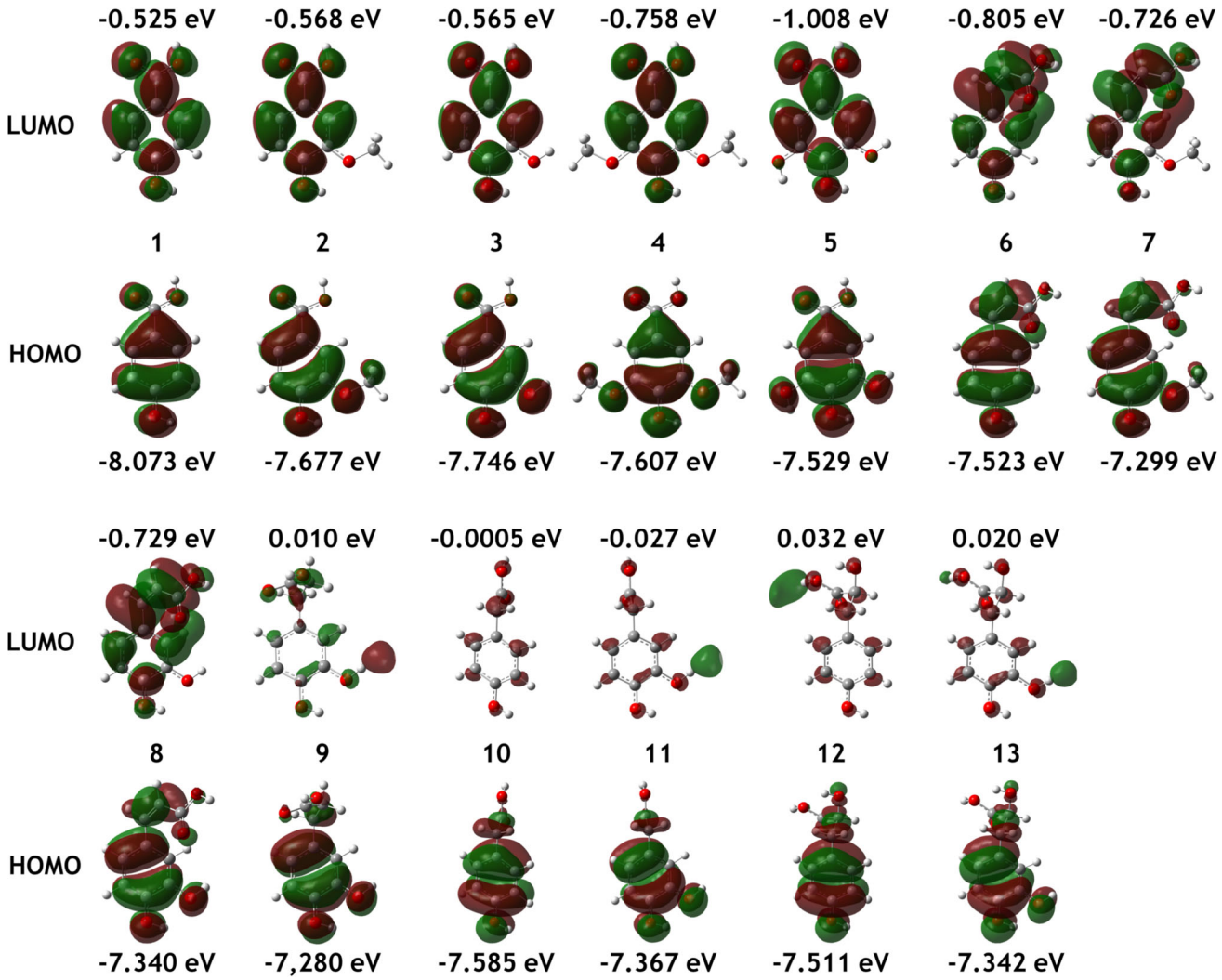

Fig. 3 Frontier orbitals ploted for the phenolic compounds using the M06-2X/6-311++G(*d,p*) level of quantum mechanics and SMD solvation model

$BDE_{molecule} - BDE_{phenol}$. Approximately 84% of the compounds in andiroba residue show improved behavior compared to phenol. Ascorbic acid, a well-known commercial antioxidant, is also used as a benchmark [43]. As shown in Fig. 4, at least 38% of the compounds resemble ascorbic acid, with energy variations around +10 kJ/mol in polar environments like water.

Among the studied compounds, molecule 9 (3,4-dihydroxyhydrocinnamic acid) exhibits the highest antioxidant potential, with hydroxyl groups at *meta* and *para* positions. In the gas phase, the relative bond dissociation energies (ΔBDE) compared to phenol are −40.8 kJ/mol (3-OH) and −4.9 kJ/mol (4-OH), indicating easier removal of the *meta*-hydrogen. However, in water, these values become nearly equivalent (−30.7 kJ/mol and −29.2 kJ/mol), suggesting hydrogen abstraction can occur at both sites.

SET-PT mechanism

As previously mentioned, the sequential electron transfer-proton transfer (SET-PT) mechanism involves transferring an electron followed by a proton to free radicals. This mechanism is characterized by ionization energy (IE) and proton dissociation energy (PDE) parameters, shown in Table 2. In the gas phase, IE values range from 756.3 to 854.6 kJ/mol, significantly higher than those for the hydrogen atom transfer (HAT) mechanism (328.8 to 379.4 kJ/mol), indicating that SET-PT is not viable for hydrogen scavenging in gaseous environments.

In the solvent, the trend persists. While proton affinities are reduced compared to the gas phase, they remain higher than those for HAT in liquid conditions. For example, in water, IP values range from 478.9 to 551.9 kJ/mol, exceeding HAT

Table 1 Bond dissociation enthalpy (BDE) and ΔBDE = $BDE_{molecule} - BDE_{phenol}$ values (kJ/mol) obtained using the M06-2X/6-311++G(*d,p*) level of theory. The results for the solvents, including the reference antioxidants, were determined using the SMD solvation model and were supplemented with experimental data (kJ/mol) as reported in the literature

Compound	Bond	BDE (kJ/mol)			ΔBDE (kJ/mol)		
		Gas	Benzene	Water	Gas	Benzene	Water
1	4-OH	379.4	379.7	394.1	9.8	11.7	17.2
2	4-OH	374.7	370.4	369.8	5.1	2.4	−7.1
3	3-OH	341.2	343.1	360.6	−28.4	−24.9	−16.3
	4-OH	376.8	372.1	371.1	7.2	4.1	−5.8
4	4-OH	356.1	351.1	350.3	−13.5	−16.9	−26.6
5	3-OH	346.4	348.5	364.6	−23.2	−19.5	−12.3
	4-OH	346.9	344.7	351.4	−22.7	−23.3	−25.5
	5-OH	379.0	373.2	372.5	9.4	5.2	−4.4
6	4-OH	368.1	361.7	372.5	−1.5	−6.3	−4.4
7	4-OH	365.9	360.6	354.7	−3.7	−7.4	−22.2
8	3-OH	345.4	344.0	360.0	−24.2	−24.0	−16.9
	4-OH	368.0	362.1	362.2	−1.6	−5.9	−14.7
9	3-OH	328.8	330.1	346.2	−40.8	−37.9	−30.7
	4-OH	364.7	357.7	347.7	−4.9	−10.3	−29.2
10	4-OH	367.7	365.7	377.8	−1.9	−2.3	0.9
11	3-OH	334.8	335.1	347.8	−34.8	−32.9	−29.1
	4-OH	368.7	361.4	355.5	−0.9	−6.6	−21.4
12	4-OH	366.5	364.2	370.8	−3.1	−3.8	−6.1
13	3-OH	333.5	334.4	348.7	−36.1	−33.6	−28.2
	4-OH	367.6	361.0	353.9	−2.0	−7.0	−23.0
Reference antioxidants							
Phenol			369.6	368.0	376.9		
Ascorbic acid			332.5	331.6	341.7		
Experimental							
Compound 4			343.5* [50]				
Compound 5			338.9* [50]; 347.4** [51, 52]				
Compound 8			339.8** [51, 52]				

*Acrylonitrile/chlorobenzene determined through the electron paramagnetic resonance spectroscopy (EPR); **Methyl linoleate/micelles estimated from the kinetic data

values (330.1 to 394.1 kJ/mol). Thus, SET-PT is not feasible, even in a solvent.

Table 4 allows a direct comparison with phenol, aiding in classifying compound performance. In the gas phase, phenol's reference value (1446.7 kJ/mol) exceeds all andiroba biomass components. Compound 5, with a gas-phase acidity of 1371.3 kJ/mol at the *meta*-position (3-OH group), shows the best chelating behavior, while others underperform compared to phenol. However, blending this material could enhance metal chelation through synergistic effects.

In the solvent, the difference is more pronounced. In water, except for compound 11, acidity values at *meta* and *para* positions are lower than phenol's ($\Delta G_{acidity}$ = 1211.2 kJ/mol).

SPLET mechanism

The sequential proton loss electron transfer (SPLET) mechanism is the final antioxidant pathway analyzed. Proton affinity (PA) governs proton abstraction and is crucial for SPLET occurrence. According to gas-phase results (Table 3), PA values are significantly higher than bond dissociation energies (BDEs), making SPLET unsuitable for hydrogen abstraction in gaseous environments.

Increasing solvent polarity from gas to aqueous conditions reduces PA values, enabling proton abstraction. For example, for compound 1, gas-phase BDE and PA values are 379.4 kJ/mol and 1391.6 kJ/mol, respectively. In benzene, these values converge to 379.7 kJ/mol (BDE) and 410 kJ/mol (PA). However, in water, the order inverts, with BDE at 394.1 kJ/mol and PA at 132.6 kJ/mol. This trend, illustrated in Fig. 5, applies to all studied molecules. Since benzene retains gas-phase behavior, SPLET occurrence clearly depends on solvent polarity.

With proton loss feasible in polar solvents, it is essential to assess electron transfer (ETE) conditions. Table 3 shows that ETE values are slightly higher than PA but comparable

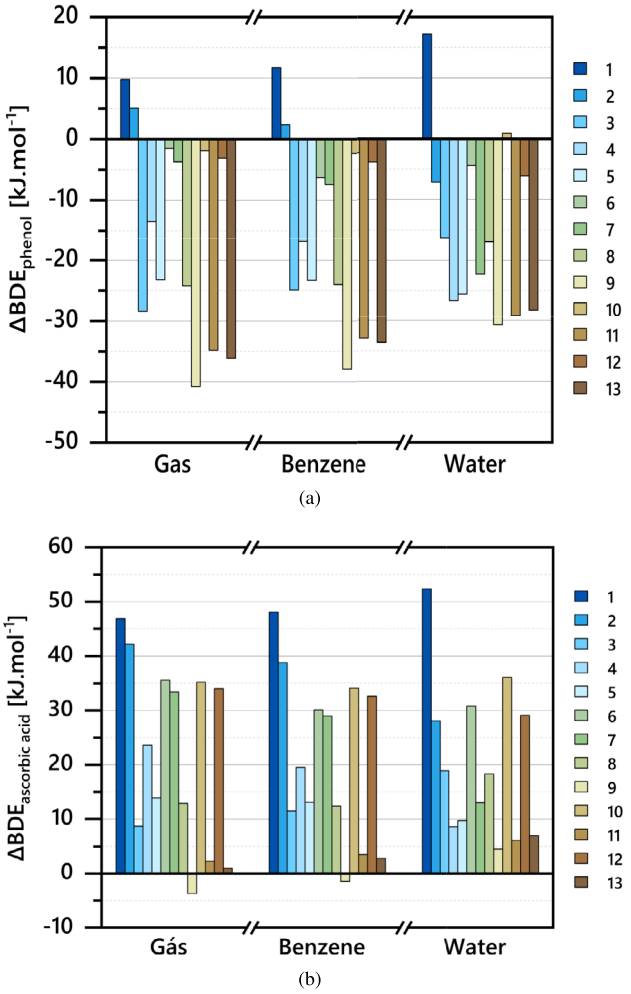

Fig. 4 Relative bond dissociation energy (ΔBDE = BDE_{mol} - BDE_{ref} calculated using phenol (**a**) and ascorbic acid (**b**) as patterns. Negative values means improved performance against the reference molecule

to BDEs, indicating that the second step of SPLET can also occur.

Metal chelating properties

The chelating ability of a compound is typically determined by analyzing its acidities, $\Delta H_{acidity}$ (gas phase) and $\Delta G_{acidity}$ (solvent) [13, 44]. These parameters measure the ease of proton removal from a neutral molecule, with lower values indicating better chelating behavior. Table 4 presents the results for phenolic compounds found in andiroba agro-industrial waste.

Under gas-phase conditions, DFT results show that acidity at the *meta* position is higher than at the *para* position. For example, compound 3 exhibits acidities of 1376.9 kJ/mol (*meta*) and 1404.5 kJ/mol (*para*), a trend consistent across all molecules. This suggests that *meta* hydroxyls favor metal chelation in phenols. This preference remains unchanged in solvent, but the environment provides an additional advantage: solute-solvent interactions reduce molecular acidity compared to gas-phase values ($\Delta H_{acidity} > \Delta G_{acidity}$). For instance, in benzene, $\Delta G_{acidity}$ decreases by approximately 100 kJ/mol relative to gas-phase results. Further increasing solvent polarity enhances acidity even more, with values around 200 kJ/mol lower than in the gas phase.

Table 4 shows that $\Delta G_{acidity}$ ranges from 1284.1 kJ/mol to 1355.2 kJ/mol in benzene and from 1179 kJ/mol to 1218.7 kJ/mol in water. These values are significantly lower than those previously reported [13, 44], confirming that andiroba biomass is a promising source of chelating molecules.

Concerning the theory-experiment agreement, Beltrán and co-workers investigated the pK_a of various polyphenolic compounds using different techniques [45]. After analyzing *p*-Hydroxybenzoic acid (1), Vanillic acid (2), Protocatechuic acid (3), Gallic acid (5), *p*-Coumaric acid (6), Ferulic acid (7), and Caffeic acid (8) acids via liquid chromatography, the authors obtained the following order for pK_a: $5 < 1 < 3 < 2 < 7 < 8 < 6$. Since this property is proportional to the Gibbs free energy ($\Delta G = 2.3RTpK_a$), it provides a connection with the theoretical results shown in Table 4. The M06-2X/6-311++G(d, p) data predicts $5 < 1 < 3 < 2 < 7 < 8 < 6$, in agreement with experimental findings.

On the other hand side,The M06-2X/6-311++G(d, p) method typically exhibits errors in predicting bond dissociation energies (BDEs), ΔG, and ΔH for aromatic compounds in the range of ±3–8 kcal/mol (~12–34 kJ/mol), depending on the bond type and system studied. For C–H bonds in aromatic hydrocarbons, errors tend to fall on the lower end (~3–5 kcal/mol), whereas bonds involving heteroatoms (O–H in phenols or N–H in anilines) may show larger deviations (5–8 kcal/mol) due to challenges in modeling charge delocalization in transition states or radical fragments.

As a particular example, using Gaussian-4 theory and M06-2X/6-311+G($3df$, $2p$) calculations, Alvareda and collaborators [46] investigated the thermochemistry and C–OH bond cleavage in flavonoids (quercetin, fisetin, luteolin) and phenolic acids (caffeic acid, pinocembrin, *p*-coumaric acid). While M06-2X showed good agreement with G4 for the weakest O–H BDEs, the mean absolute deviation (MAD) between methods was 5.0 kcal/mol for BDEs and 10.0 kcal/mol for ΔH. With better results, Hou and You investigated the reaction kinetics of hydrogen abstraction from polycyclic aromatic hydrocarbons by H atoms, obtaining a MAD value of 1.0 kcal/mol using M06-2X/6-311 g(d, p) in comparison with CCSD(T)/CBS calculations [47].

Hydrogen abstraction by hydroxyl radicals

Our thermochemical and electronic structure analysis enables the determination of the best antioxidant performances

Table 2 Ionization energy (IE) and proton dissociation enthalpy (PDE) values were calculated using the M06-2X/6-311++G(p, d) theoretical level. The simulations were conducted in the gas phase, in nonpolar and polar environments in the SMD solvation model

Bond	IE (kJ/mol)			PDE (kJ/mol)			SET-PT (kJ/mol)		
	Gas	Benzene	Water	Gas	Benzene	Water	Gas	Benzene	Water
1	854.6	720.0	551.9						
4-OH				836.0	72.9	5.3	1690.6	792.9	557.2
2	797.1	669.2	507.7						
4-OH				888.7	114.4	25.2	1685.8	783.6	532.9
3	817.9	687.5	517.0						
3-OH				834.4	68.7	6.7	1652.3	756.2	523.7
4-OH				870.0	97.8	17.1	1687.9	785.3	534.1
4	763.6	644.2	498.5						
4-OH				903.6	120.0	14.8	1667.2	764.2	513.3
5	813.4	688.8	516.8						
3-OH				844.1	72.9	10.9	1657.5	761.7	527.7
4-OH				844.6	69.1	−2.3	1658.0	757.9	514.5
5-OH				876.7	97.6	18.7	1690.1	786.4	535.5
6	788.9	661.3	508.6						
4-OH				890.3	113.5	27.0	1679.2	774.8	535.6
7	756.3	638.0	487.0						
4-OH				920.8	135.7	30.9	1677.1	773.7	517.9
8	722.6	650.6	492.3						
3-OH				883.9	106.5	30.7	1606.5	757.1	523.0
4-OH				906.5	124.6	33.0	1629.1	775.2	525.3
9	755.7	634.2	478.9						
3-OH				884.3	109.0	30.4	1640.0	743.2	509.3
4-OH				920.2	136.6	31.9	1675.9	770.8	510.8
10	801.3	668.3	512.2						
4-OH				877.6	110.5	28.7	1678.9	778.8	540.9
11	774.1	649.6	491.6						
3-OH				871.9	98.6	19.2	1646.0	748.2	510.8
4-OH				905.8	124.9	26.9	1679.9	774.5	518.5
12	781.9	662.1	505.6						
4-OH				895.7	115.2	28.3	1677.6	777.3	533.9
13	757.8	655.5	481.7						
3-OH				886.8	92.1	30.0	1644.6	747.6	511.7
4-OH				920.9	118.6	35.3	1678.7	774.1	517.0
Reference Antioxidants									
Phenol	824.3	683.6	518.1	856.4	97.5	21.9	1680.7	781.1	540.0
Ascorbic acid	833.4	706.1	521.4	810.3	38.7	−16.6	1643.7	744.8	504.8

among the thirteen compounds found in andiroba waste, as well as the preferential molecular site for hydrogen abstraction. However, the mechanism of radical inhibition can only be fully understood by explicitly considering the interactions between the reference molecule and the free radical.

This goal can be achieved by starting from reactant (RE) and product (PR) configurations and generating transition state (TS) structures. The difference between the single-point energy of the transition state and the reactants ($E_a = TS - RE$) provides the energy barrier (see Fig. 6) that must be overcome in the chemical reaction. Table 5 presents these parameters for compounds 11 and 13 inhibiting OH radicals. In addition, all values account for zero-point energy (ZPE) corrections. Thus, the energy of transition state energy is the sum of the electronic energy and ZPV corrections ($E_{TS}^{ZPE} = E_{TS}^{electronic} + E_{ZPE}^{TS}$), and the activation energy is $E_a = E_{TS}^{ZPE} - E_{RE}^{ZPE}$.

First, by analyzing the ωB97XD results, the superior performance of molecule 13 is confirmed. According to DFT calculations, the energy barrier estimated for this compound

Table 3 Proton affinities (PA) and electron transfer enthalpies (ETE) values with M06-2X/6-311++G(p, d) level of theory. The results for the solvents, including the reference antioxidants, were determined using the SMD solvation model

Bond	PA (kJ/mol)			ETE (kJ/mol)			SPLET (kJ/mol)		
	Gas	Benzene	Water	Gas	Benzene	Water	Gas	Benzene	Water
1									
4-OH	1391.6	410.0	132.6	299.0	382.9	424.5	1690.6	792.9	557.1
2									
4-OH	1413.4	429.5	132.3	272.5	354.0	400.5	1685.9	783.5	532.8
3									
3-OH	1383.1	404.0	131.0	269.3	352.2	392.7	1652.4	756.2	523.7
4-OH	1410.7	426.6	131.7	277.3	358.7	402.4	1688.0	785.3	534.1
4									
4-OH	1417.8	435.2	130.5	249.4	329.0	382.9	1667.2	764.2	513.4
5									
3-OH	1377.5	398.4	129.9	280.0	363.2	397.8	1657.5	761.6	527.7
4-OH	1381.9	399.8	120.2	276.1	358.0	394.3	1658.0	757.8	514.5
5-OH	1436.5	398.4	142.9	253.6	387.9	392.6	1690.1	786.3	535.5
6									
4-OH	1384.7	408.4	139.1	294.6	366.4	396.5	1679.3	774.8	535.6
7									
4-OH	1404.9	426.0	137.1	272.2	347.8	380.8	1677.1	773.8	517.9
8									
3-OH	1396.4	416.4	139.0	260.1	340.8	384.1	1656.5	757.2	523.1
4-OH	1401.1	419.2	137.3	278.0	356.0	388.0	1679.1	775.2	525.3
9									
3-OH	1401.0	418.5	141.7	239.0	324.6	367.6	1640.0	743.1	509.3
4-OH	1462.1	467.4	156.9	213.7	303.4	353.8	1675.8	770.8	510.7
10									
4-OH	1432.3	446.9	157.5	244.6	331.9	383.5	1676.9	778.8	541.0
11									
3-OH	1399.8	417.4	141.9	246.2	330.8	369.0	1646.0	748.2	510.9
4-OH	1455.2	464.4	156.5	224.7	310.0	362.0	1679.9	774.4	518.5
12									
4-OH	1435.2	450.0	154.0	242.4	327.3	379.9	1677.6	777.3	533.9
13									
3-OH	1396.9	418.4	138.6	247.8	329.2	373.1	1644.7	747.6	511.7
4-OH	1455.3	465.3	153.4	223.4	308.8	363.6	1678.7	774.1	517.0
Reference Antioxidants									
Phenol	1452.9	453.8	154.3	227.9	327.3	385.7	1680.8	781.1	540.0
Ascorbic acid	1312.7	344.0	87.4	331.0	400.8	417.4	1643.7	744.8	504.8

is 1.94 kJ/mol, which is slightly lower than that reported for the second molecule, 2.21 kJ/mol. Although the differences are subtle (0.27 kJ/mol), they confirm the predictions made using thermochemical analysis.

In line with the quantum mechanical framework, we verified the influence of Hartree-Fock exchange-correlation and dispersion corrections, which have become popular in DFT. Our ωB96 calculations, which do not account for these corrections, point out activation energies of 6.38 kJ/mol and 6.03 kJ/mol, respectively, for molecules 11 and 13. These values are three times those reported by the ωB97XD version, providing a poor description of the phenomenon.

We also tested the performance of CAM-B3LYP, which includes long-range corrections and some portions of Hartree-Fock exchange, but is not about the dispersion force. In such a case, we obtained transition barriers of 2.01 kJ/mol and 1.81 kJ/mol, respectively, for molecules 11 and 13, showing good agreement with ωB97XD data. This finding indicates

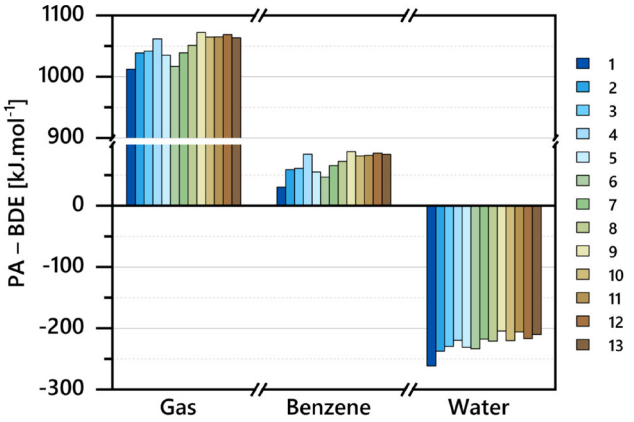

Fig. 5 Difference between the proton affinity (PA) and bond dissociation energy (BDE). Negative values means improved performance against the reference molecule

that the exchange-correlation effects can be more relevant for describing TS energies.

The poorest description for both compounds comes from the ωB97 method. Although this Hamiltonian model accounts for long-range corrections, it does not include any dispersion correction. Thus, at first glance, one might assume that dispersion forces are essential for describing the phenolic compounds under investigation. However, considering the results for compound 11, the differences between CAM-B3LYP and ωB97XD are minor. This suggests that the absence of dispersion corrections is not the main issue. Consequently, we conclude that using ωB97 to investigate transition states involving phenolic compounds and free radicals may be unreliable. Similar conclusions apply to compound 13.

The impact also arises at the structure of the TS. For example, from Fig. 7, the evolution of the $r(\mathrm{O}\cdots\mathrm{H})$, $r(\mathrm{O}-\mathrm{H})$, and $\theta(\mathrm{OHO})$ parameters for molecule 11 can be analyzed at different DFT levels. If one uses the ωB97 functional, which lacks a portion of pure Hartree-Fock exchange and dispersion corrections, the obtained values are 1.32 Å, 1.08 Å, and 159.7° for $r(\mathrm{O}\cdots\mathrm{H})$, $r(\mathrm{O}-\mathrm{H})$, and $\theta(\mathrm{OHO})$, respectively. In contrast, when both corrections are included using the ωB97XD method, the values shift slightly to 1.39 Å, 1.05 Å, and 162.4° (see Fig. 7). Clearly, these changes are significant and can not be neglected.

Regarding other dyes, these compounds present competitive behavior. Also at gas phase conditions, there have been reported energy barriers varying from 19 kJ/mol to 21.6 kJ/mol for a new class of xanthones recently found in the endophytic fungus *Guignardia mangiferae* [18]. For scopolin, a natural antioxidant compound belonging to the coumarin class, activation energies of 20.91 kcal/mol have been reported [20] (These values do not account for ZPE corrections).

However, analyzing the energy barrier alone is insufficient to fully understand the reaction pathway. This task is better accomplished using the intrinsic reaction coordinate (IRC) concept [48, 49], which connects reactants, transition states, and products (see Fig. 8).

The key parameter in such cases is the activation energy ($E_a = E_{\mathrm{TS}} - E_{\mathrm{RE}}$). The lower E_a, the easier and faster the reaction proceeds. For compound 13, $E_a = 5.8 \times 10^{-3}$ Hartree is less than that reported for its counterpart (44.9×10^{-3} Hartree), indicating that the antioxidant reaction initiates and completes more easily.

Table 4 $\Delta H_{acidity}$ (kJ/mol) and $\Delta G_{acidity}$ (kJ/mol) values were calculated using the DFT/M06-2X/6-311++G(d, p) theoretical level. The simulations were conducted in the gas phase, in nonpolar and polar environments in the SMD solvation model

Bond	$\Delta H_{acidity}$ Gas	$\Delta G_{acidity}$ Benzene	pK_a* exp. Water	[45]
1				4.7
4-OH	1385.4	1286.8	1189.3	
2				4.7
4-OH	1407.2	1309.2	1190.6	
3				4.7
3-OH	1376.9	1284.3	1189.3	
4-OH	1404.5	1304.7	1189.4	
4	4-OH	1411.6	1311.8	1190.1
5				4.5
3-OH	1371.3	1285.2	1188.0	
4-OH	1375.7	1284.1	1179.0	
5-OH	1430.3	1325.6	1201.9	
6				4.8
4-OH	1378.5	1288.3	1202.8	
7				4.8
4-OH	1398.7	1310.2	1200.3	
8	3-OH	1390.2	1299.1	1203.4
4-OH	1394.9	1306.0	1201.9	
9				4.8
3-OH	1401.0	1298.3	1197.7	
4-OH	1462.1	1350.8	1211.4	
10	4-OH	1434.3	1329.1	1218.7
11	3-OH	1393.6	1301.3	1203.0
4-OH	1449.0	1345.6	1214.9	
12	4-OH	1429.0	1331.0	1209.9
13	3-OH	1390.7	1302.0	1195.9
4-OH	1449.1	1355.2	1209.4	
	Phenol	1446.7	1331.1	1211.2

*Liquid chromatography in water (10% MeCN)

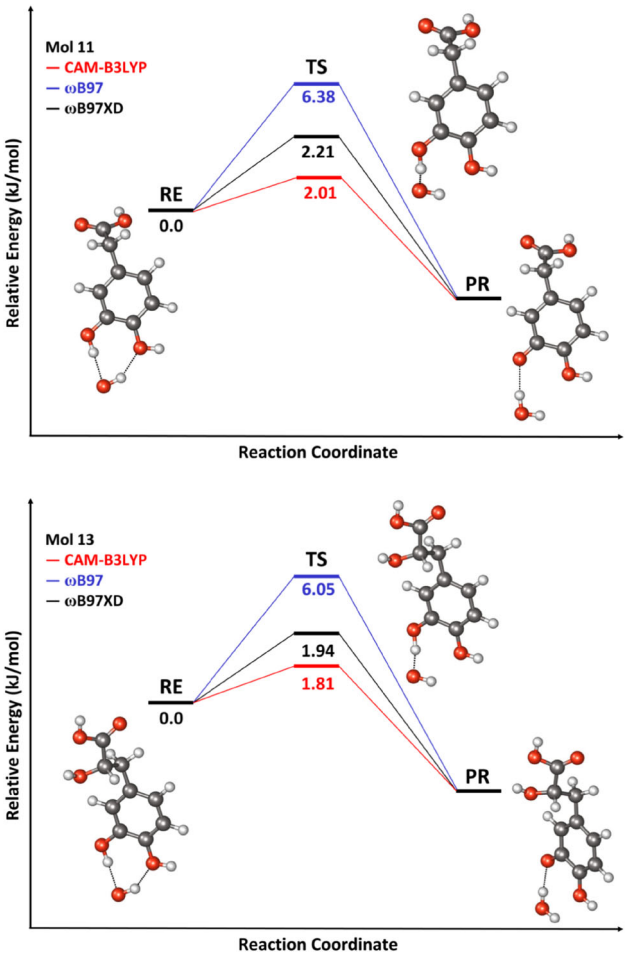

Fig. 6 The gas phase barriers of energy necessary for the chemical reactions between OH radicals and molecules 11 (top) and 13 (bottom), respectively. This values include zero-point energy (ZPE) corrections

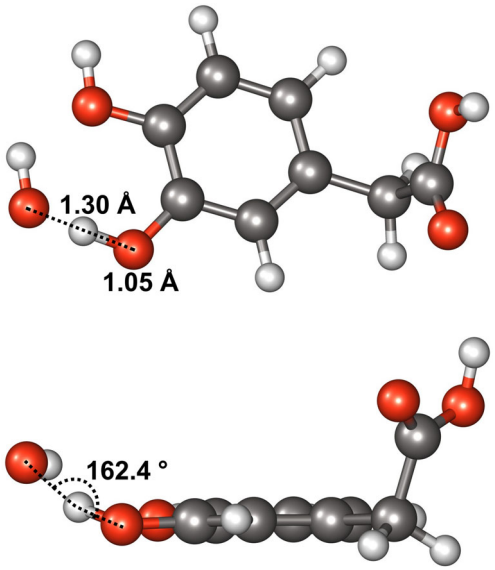

Fig. 7 Front and side views of transition states calculated for compound 11 interacting with the OH radical. The geometries were calculated at the gas phase at ωB97XD/6-31+G(d) level of quantum mechanics. The parameters are $r(\mathrm{O}\cdots\mathrm{H}) = 1.30$ Å, $r(\mathrm{O}-\mathrm{H}) = 1.05$ Å, and $\theta = (\mathrm{OHO}) = 162.4°$

Conclusions

Using density functional theory (DFT), this work investigates the hydrogen scavenging process in thirteen phenolic compounds from *Carapa guianensis* agro-industrial waste. This analysis is crucial for understanding the antioxidant mechanisms of chromophores and their applications as metal chelators, which are vital in cosmetics to prevent stability issues.

Quantum mechanical calculations show that the position of OH groups on the aromatic ring significantly influences hydrogen and proton abstraction. DFT analysis of molecular enthalpies and Gibbs free energies reveals that hydrogen and proton removal is easier from OH groups at the *meta* position across all studied molecules.

Regarding antioxidant efficiency, approximately 85% of the phenolic derivatives in *Carapa guianensis* waste exhibit competitive hydrogen dissociation energies compared to phenol. However, only 35% are competitive with ascorbic acid, a commercial antioxidant standard. Among these, three

Table 5 The relative energies for the reaction barrier (TS-RE), products (PR-RE), as well as structural parameters calculated for the optimized reactants, transition states, and products at gas phase conditions

	Mol 11			Mol 13		
	CAM-B3LYP	ωB97	ωB97XD	CAM-B3LYP	ωB97	ωB97XD
Energy Barrier (TS-RE)	2.01	6.38	2.21	1.81	6.05	1.94
PR-RE	−30.78	−31.62	−31.42	−31.21	−32.02	−32.13
$r(\mathrm{O}-\mathrm{H})$	1.06	1.08	1.05	1.05	1.07	1.04
$r(\mathrm{O}\cdots\mathrm{H})$	1.38	1.32	1.39	1.39	1.33	1.40
θ(OHO)	164.2	159.7	162.4	163.8	159.7	162.1

All values were corrected for zero-point energy (ZPE) contributions, and the calculations were carried out using the unrestricted CAM-B3LYP, ωB97, and ωB97XD methods associated with the 6-31+G(d) basis set. Energies are in kJ/mol, bonds and angles are in angstroms and degrees, respectively

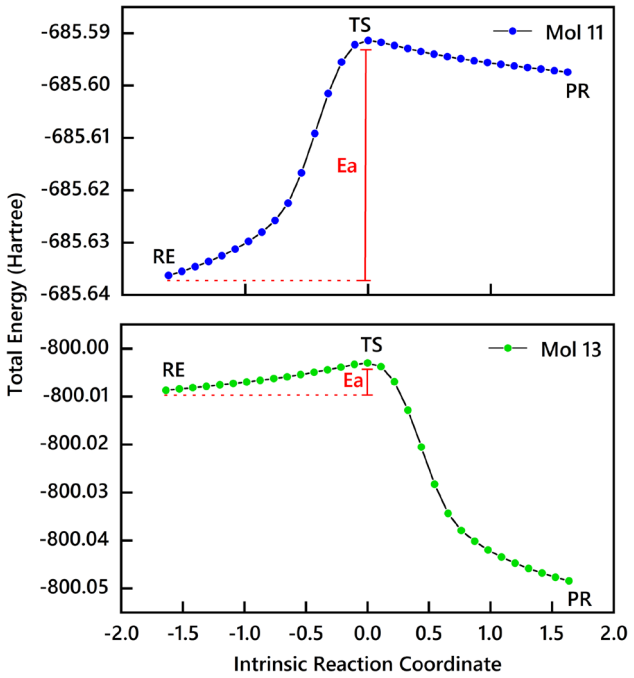

Fig. 8 Intrinsic reaction coordinate (IRC) paths calculated for using the ωB97XD method for molecules 11 (top) and 13 (bottom) at the gas phase

chromophores (9, 11, and 13) show slight energetic deviations from ascorbic acid, highlighting the waste's potential as a source of potent antioxidants.

Solvent effects, modeled using continuum approaches, significantly influence antioxidant behavior. While solvents typically facilitate hydrogen dissociation, some compounds exhibit altered behavior as polarity increases from benzene to water. Thus, solvent selection is critical to maximizing antioxidant potential. Additionally, the solvent enhances metal chelation performance compared to gas-phase conditions.

Beyond altering hydrogen dissociation energies, the solvent also affects the antioxidative mechanism. From the gas phase to benzene, hydrogen removal energy decreases, but the hydrogen atom transfer (HAT) mechanism remains dominant. In highly polar solvents like water, the mechanism shifts to sequential proton loss electron transfer (SPLET), underscoring the importance of solvent polarity.

The analysis of the mechanism of hydrogen scavenging by explicit hydroxyl radicals confirms the order of the antioxidant power of the investigated compounds. Moreover, this analysis reinforces the importance of including Hartree-Fock exchange-correlation contribution, once the in the absence of these interactions it is not possible to describe correctly these properties.

Supplementary Information The online version contains supplementary material available at https://doi.org/10.1007/s00894-025-06517-2.

Author contributions Neidy S. S. dos Santos: electronic structure calculations, data analysis, writing. Loubenky Surfin: electronic structure calculations, data analysis, writing. William Silva: electronic structure calculations, data analysis, writing. Antônio R. da Cunha: formal analysis, writing original draft. Herbert Georg: formal analysis, writing original draft. Kaline Coutinho: writing review and editing, supervision. Sylvio Canuto: writing original draft, writing review and editing, supervision. Rodrigo Gester: writing original draft, writing review and editing, supervision.

Data availability No datasets were generated or analysed during the current study.

Declarations

Competing interests The authors declare no competing interests.

References

1. Rozantsev EG, Loshadkin DV (2001) The history and modern problems of free radical chemistry. 100 years of free radical chemistry. Des Monomers Polym 4:281–300. https://doi.org/10.1163/156855501753210781
2. Zwart LL, Meerman JHN, Commandeur JNM, Vermeulen NPE (1999) Biomarkers of free radical damage: applications in experimental animals and in humans. Free Radic Biol Med 26:202–226. https://doi.org/10.1016/S0891-5849(98)00196-8
3. Krishnaiah D, Sarbatly R, Nithyanandam R (2011) A review of the antioxidant potential of medicinal plant species. Food Bioprod Process 89:217–233. https://doi.org/10.1016/j.fbp.2010.04.008
4. Mahongnao S, Sharma P, Nanda S (2023) Conversion of waste materials into different by-products of economic value. In: Singh P, Verma P, Singh R, Ahamad A, Batalhão ACS (eds) Waste Manag Resour Recycling Dev World. pp 665–699. https://doi.org/10.1016/B978-0-323-90463-6.00030-0
5. Lade VG, Mahajan KP, Rukhane PV (2023) Technologies for the production of value-added products from agro-wastes and their possible applications. In: Raut NA, Kokare DM, Bhanvase BA, Randive KR, Dhoble SJ (eds) 360-Degree Waste Manag 1:39–66. https://doi.org/10.1016/B978-0-323-90760-6.00007-2
6. Sadh PK, Duhan S, Duhan JS (2018) Agro-industrial wastes and their utilization using solid-state fermentation: a review. Bioresour Bioprocess 5:1–15. https://doi.org/10.1186/s40643-017-0187-z
7. Soares AS, Wanzeler AMV, Cavalcante GHS, Barros EMS, Carneiro RCM, Tuji FM (2021) Therapeutic effects of andiroba (Carapa guianensis Aubl) oil, compared to low power laser, on oral mucositis in children underwent chemotherapy: a clinical study. J Ethnopharmacol 264. https://doi.org/10.1016/j.jep.2020.113365
8. Fonseca ASA, Monteiro IS, Santos CR, Carneiro MLB, Morais SS, Araújo PL, Santana TF, Joanitti GA (2024) Effects of andiroba oil (Carapa guianensis Aublet) on the immune system in inflammation and wound healing: a scoping review. J Ethnopharmacol 327. https://doi.org/10.1016/j.jep.2024.118004
9. Wanzeler AMV, Júnior SMA, Gomes JT et al (2018) Therapeutic effect of andiroba oil (Carapa guianensis Aubl) against oral mucosi-

tis: an experimental study in golden Syrian hamsters. Clin Oral Invest 22:2069–2079. https://doi.org/10.1007/s00784-017-2300-2
10. Oliveira FR, Rodrigues KE, Hamoy M, Sarquis IR, Hamoy AO, Lopez MEC, Ferreira IM, Macchi BM, Nascimento JLM (2020) Fatty acid amides synthesized from andiroba oil (Carapa guianensis Aublet) exhibit anticonvulsant action with modulation on GABA-A receptor in mice: a putative therapeutic option. Pharm 13:43. https://doi.org/10.3390/ph13030043
11. Santos KIP, Benjamim JKF, Costa KAD, Reis AS, Pinheiro WBS, Santos AS (2021) Metabolomics techniques applied in the investigation of phenolic acids from the agro-industrial by-product of Carapa guianensis Aubl. Arab J Chem 14. https://doi.org/10.1016/j.arabjc.2021.103421
12. Fonseca S, Santos NSS, Torres A, Siqueira M, Cunha A, Manzoni V, Provasi PF, Gester R, Canuto S (2023) The role of the solvent and intramolecular hydrogen bonds in the antioxidative mechanism of prenylisoflavone from leaves of Vatairea guianensis. J Phys Chem A 127:10807–10816. https://doi.org/10.1021/acs.jpca.3c05725
13. Urbaniak A, Szela M, Molski M (2013) Theoretical investigation of stereochemistry and solvent influence on antioxidant activity of ferulic acid. Comput Theor Chem 1012:33–40. https://doi.org/10.1016/j.comptc.2013.02.018
14. Urbaniak A, Kujawski J, Czaja K, Szelag M (2017) Antioxidant properties of several caffeic acid derivatives: a theoretical study. C R Chim 20:1072–1082. https://doi.org/10.1016/j.crci.2017.08.003
15. Saeidian H, Bakhtiari A, Mirjafary Z, Larijani K (2024) DFT investigation of physicochemical and antioxidant properties of fluorinated flavones. Struct Chem 35:1199–1213. https://doi.org/10.1007/s11224-023-02258-1
16. Boulmokh Y, Belguidoum K, Meddour F, Amira-Guebailia H (2024) Enhanced antioxidant properties of novel curcumin derivatives: a comprehensive DFT computational study. Struct Chem 35:825–839. https://doi.org/10.1007/s11224-023-02237-6
17. Tenorio FJ (2024) Hernandez da (2024) conceptual DFT study of antioxidant activity of carotenoids and its radicals. Struct Chem. https://doi.org/10.1007/s11224-024-02429-8
18. Santos NSS, Barbieri HB, Pinheiro M, Fill TP, Queiroz MH, Pina J, Belo E, Georg HC, da Cunha AR, Marinho PSB, Marinho AMR, Coutinho K, Canuto S, Gester R (2024) Theoretical and experimental study of a new antioxidant xanthone: solvent and intramolecular hydrogen bond effects. J Mol Liq 408:125045. https://doi.org/10.1016/j.molliq.2024.125045
19. dos Santos NSS (2024) Molecular modeling of antioxidant and non-linear optical properties of organic compounds. Dissertation, Universidade Federal do Sul e Sudeste do Pará. https://ri.unifesspa.edu.br//handle/123456789/2111
20. Karunarathna BSW, Gajasinghe GMST, Wanniarachchi GKK, Seneweera S (2024) A DFT analysis of the antioxidant capacity of scopolin and scopoletin. J Mol Model 30:424. https://doi.org/10.1007/s00894-024-06192-9
21. Badeji AA, Omoniyi MT, Ogunbayo TB et al (2024) Quantum chemical investigation of the degradation of acid orange 7 by different oxidants. Discov Chem 1:55. https://doi.org/10.1007/s44371-024-00059-x
22. Aydogdu S, Hatipoglu A (2023) Theoretical insights into the reaction mechanism and kinetics of ampicillin degradation with hydroxyl radical. J Mol Model 29:63. https://doi.org/10.1007/s00894-023-05462-2
23. Aydogdu S, Hatipoglu A (2023) Aqueous degradation of 6-APA by hydroxyl radical: a theoretical study. J Mol Model 29:222. https://doi.org/10.1007/s00894-023-05636-y
24. Mahmoudi S, Dehkordi MM, Asgarshamsi MH (2021) Density functional theory studies of the antioxidants–a review. J Mol Model 27:271. https://doi.org/10.1007/s00894-021-04891-1
25. Bartmess JE (1994) Thermodynamics of the electron and the proton. J Phys Chem 98(25):6420–6424. https://doi.org/10.1021/j100076a029
26. Marković Z, Tošović J, Milenković D, Marković S (2016) Revisiting the solvation enthalpies and free energies of the proton and electron in various solvents. Comput Theor Chem 1077:17. https://doi.org/10.1016/j.comptc.2015.09.007
27. Leopoldini M, Russo N, Toscano M (2011) The molecular basis of working mechanism of natural polyphenolic antioxidants. Food Chem 125:288. https://doi.org/10.1016/j.foodchem.2010.08.012
28. Martins HFP, Leal JP, Fernandez MT, Lopes VHC, Cordeiro MND (2004) Toward the prediction of the activity of antioxidants: experimental and theoretical study of the gas-phase acidities of flavonoids. J Am Soc Mass Spectrom 15:848–861. https://doi.org/10.1016/j.jasms.2004.02.007
29. Souza GLC, Peterson KA (2021) Benchmarking antioxidant-related properties for gallic acid through the use of DFT, MP2, CCSD, and CCSD(T) approaches. J Phys Chem A 125:198–208. https://doi.org/10.1021/acs.jpca.0c09116
30. Marenich AV, Cramer CJ, Truhlar DG (2009) Universal solvation model based on solute electron density and a continuum model of the solvent defined by the bulk dielectric constant and atomic surface tensions. J Phys Chem B 113:6378–6396. https://doi.org/10.1021/jp810292n
31. Francisco-Márquez M, Galano A (2019) Detailed investigation of the remarkable peroxyl radical scavenging activity of two new aminopyridinol-based compounds. J Chem Inf Model 59(8):3494–3505. https://doi.org/10.1021/acs.jcim.9b00517
32. Biela M, Kleinová A, Klein E (2022) Phenolic acids and their carboxylate anions: thermodynamics of primary antioxidant action. Phytochem 200:113254. https://doi.org/10.1016/j.phytochem.2022.113254
33. Peng C, Schlegel HB (1993) Combining synchronous transit and quasi-newton methods for finding transition states. Israel J Chem 33:449–454. https://doi.org/10.1002/ijch.199300051
34. Goerigk L, Hansen A, Bauer C, Ehrlich S, Najibi A, Grimme S (2017) A look at the density functional theory zoo with the advanced GMTKN55 database for general main group thermochemistry, kinetics and noncovalent interactions. Phys Chem Chem Phys 19:32184–32215. https://doi.org/10.1039/C7CP04913G
35. Souza GLC, Peterson KA (2021) Benchmarking antioxidant-related properties for gallic acid through the use of DFT, MP2, CCSD, AND CCSD(T) approaches. J Phys Chem A 125:198–208. https://doi.org/10.1021/acs.jpca.0c09116
36. Goerigk L, Grimme S (2011) A thorough benchmark of density functional methods for general main group thermochemistry, kinetics, and noncovalent interactions. Phys Chem Chem Phys 13:6670–6688. https://doi.org/10.1039/C0CP02984J
37. Frisch MJ, et al. (2016) Gaussian 16, Revision C.01. Gaussian Inc. Wallingford CT
38. Parkinson CJ, Mayer PM, Radom L (1999) An assessment of theoretical procedures for the calculation of reliable radical stabilization energies. J Chem Soc 11:2305. https://doi.org/10.1039/A905476F
39. Boulebd H (2020) Comparative study of the radical scavenging behavior of ascorbic acid, BHT, BHA and Trolox: experimental and theoretical study. J Mol Struct 1201. https://doi.org/10.1016/j.molstruc.2019.127210
40. Guedes RC, Coutinho K, Costa Cabral BJ, Canuto S (2003) Differential hydration of phenol and phenoxy radical and the energetics of the phenol o-h bond in solution. J Phys Chem B 107(18):4304–4310. https://doi.org/10.1021/jp0219449
41. Guedes RC, Coutinho K, Costa Cabral BJ, Canuto S, Correia CF, Borges dos Santos RM, Martinho Simões JA (2003) Solvent effects on the energetics of the phenol o-h bond: differential solvation of phenol and phenoxy radical in benzene and acetonitrile. J Phys Chem A 107(43):9197–9207. https://doi.org/10.1021/jp035912c

42. Xue YS, Zheng YW, An L, Dou Y, Liu Y (2014) Density functional theory study of the structure–antioxidant activity of polyphenolic deoxybenzoins. Food Chem 151:198–206. https://doi.org/10.1016/j.foodchem.2013.11.064
43. Mat A, Ismail A, Bahareh S (2016) Ascorbic acid: physiology and health effects. Encycl Food Health:266–274. https://doi.org/10.1016/b978-0-12-384947-2.00045-3
44. Leopoldini M, Russo N, Toscano M (2011) The molecular basis of working mechanism of natural polyphenolic antioxidants. Food Chem 125:288–306. https://doi.org/10.1016/j.foodchem.2010.08.012
45. Beltrán JL, Sanli N, Fonrodona G, Barrón D, Özkan G, Barbosa J (2003) Spectrophotometric, potentiometric and chromatographic pKa values of polyphenolic acids in water and acetonitrile–water media. Anal Chim Acta 484:253–264. https://doi.org/10.1016/S0003-2670(03)00334-9
46. Alvareda E, Denis PA, Iribarne F, Paulino M (2016) Bond dissociation energies and enthalpies of formation of flavonoids: a G4 and M06–2X investigation. Comput Theor Chem 1091:18–23. https://doi.org/10.1016/j.comptc.2016.06.021
47. Hou D, You X (2017) Reaction kinetics of hydrogen abstraction from polycyclic aromatic hydrocarbons by h atoms. Phys Chem Chem Phys 19:30772–30780. https://doi.org/10.1039/C7CP04964A
48. Fukui K (1981) The path of chemical reactions – the IRC approach. Acc Chem Res 14:363–368. https://doi.org/10.1021/ar00072a001
49. Hratchian HP, Schlegel HB (2005) In: Dykstra CE, Frenking G, Kim KS, Scuseria G (eds) *Theory and applications of computational chemistry: the first 40 years*. Elsevier, Amsterdam, pp 195–249
50. Alberti A, Amorati R, Campredon M, Lucarini M, Macciantelli D, Pedulli G (2009) Antioxidant activity of some simple phenols present in olive oil. Acta Aliment 38:427–436. https://doi.org/10.1556/aalim.38.2009.4.3
51. Denisova TG, Denisov ET (2008) Dissociation energies of o-h bonds in natural antioxidants. Russ J Chem Bull 57:1858–1866. https://doi.org/10.1007/s11172-008-0251-0
52. Roginsky V (2003) Chain-breaking antioxidant activity of natural polyphenols as determined during the chain oxidation of methyl linoleate in triton x-100 micelles. Arch Biochem Biophys 414(2):261–270. https://doi.org/10.1016/s0003-9861(03)00143-7